Influence of low- and high-speed structures on the quiescent core region in a turbulent pipe flow

Jongmin Yang
Department of Mechanical Engineering
KAIST
Daejeon 34141, Republic of Korea
Email : asyligo@kaist.ac.kr

Jinyul Hwang
Department of Mechanical Engineering
KAIST
Daejeon 34141, Republic of Korea
Email : j.yhwang@kaist.ac.kr

Hyung Jin Sung
Department of Mechanical Engineering
KAIST
Daejeon 34141, Republic of Korea
Email : hjsung@kaist.ac.kr

ABSTRACT

The structural organization of the quiescent core region in a turbulent pipe flow was investigated using direct numerical simulation data at Re_τ = 934. The quiescent core region was the uniform momentum zone located at the center of the pipe flow. It contained the highest streamwise momentum with a low level of turbulence. The interface of the quiescent core region could be identified from the probability density function (PDF) of the streamwise modal velocity. In the vicinity of the interface of the quiescent core region, the streamwise velocity changed abruptly. The abrupt jump in velocity caused an increase of the velocity gradient. The interface of the quiescent core region was similar to the laminar superlayer in turbulent/non-turbulent interface (TNTI). The interface of the quiescent core region contained the low- and high-speed structures. The low-speed structure was organized with relatively high interface height and sweep motion. Conversely, the high-speed structure was organized with relatively low interface height and ejection motion. The low- and high-speed structures near the core interface were divided into wall-attached and detached groups depending on the distance between the structures and the wall. Since the wall-attached groups near the interface had a huge volume, it had a large influence on the statistical amount near the interface.

INTRODUCTION

The Wall-bounded turbulent flows could be divided into an external flow and an internal flow according to geometric characteristics. According to the geometrical characteristics, the internal flow had a fully-turbulent region, whereas the external flow had an interface with non-turbulent potential flow. Turbulent entrainment behaviors, such as spreading or mixing, were observed at the interface of TBL, called the 'turbulent/non-turbulent interface (TNTI)', which was not present in internal flows. Kwon *et al*. (2014) observed an interfacial layer by using the concept of uniform momentum zone (UMZ) in turbulent channel flow and found that this interfacial layer was similar to the TNTI. The UMZ demarcates a large core region with a low-level turbulence, which they termed the quiescent core region. The TNTI played an important role in momentum and energy transfer and was attracting attention due to its various engineering applications such as growth, mixing and spreading (de Silva et al. 2014). It is important to interpret the mechanism in the quiescent core region from the perspective of TNTI models.

The presence of UMZs in a TBL was first reported by Meinhart and Adrian (1995). They identified numerous zonal structures with relatively uniform streamwise momentum. These UMZs were surrounded by thin viscous shear layers which contained spanwise vortical structures. Adrian *et al*. (2000) identified the UMZ using the probability density function (PDF) of the instantaneous streamwise velocity. These UMZs were induced from the structure called vortex packets. These vortex packets were a structure formed by the streamwise alignments of the hairpins. Due to the vortex in the head of these hairpins, the streamwise velocity changed drastically in the boundary of UMZs and a velocity gradient occurred. The streamwise velocity remained homogeneous inside UMZs and Numerous UMZs were generated by the hierarchy of the vortex packets. Kwon *et al*. (2014) applied the identification method for UMZ

using the PDF of the modal velocity in a turbulent channel flow. Modal velocities were the convection velocity that represented UMZs. The modal velocity above $0.95U_{CL}$ were robust in very long streamwise domain lengths. The consistency of these modal velocities implied the existence of a robust UMZ in the channel. The UMZ, a large core located at the center of the channel, which had a meandering feature. This core contained relatively low levels of turbulence compared to outside of the core. The large core region was termed the quiescent core region. At the interface of the core region, the shear layer was created due to the rapid change of the streamwise velocity.

The TNTI was a region where external non-turbulent and turbulent flow encountered and transport phenomena occurred. As TNTI passed through the laminar superlayer, the viscous effect decrease continuously (Corrsin and Kistler 1955) and vorticity transmission decreased. The transport mechanisms at the core interface were divided into two types according to the length scale: small-scale nibbling, or large-scale engulfment. Due to these two mechanisms, flow quantities such as mass, momentum, and other scalar values were exchanged through the TNTI region. Westerweel *et al*. (2005) and Chauhan *et al*. (2014) suggested that small-scale nibbling played a dominant role in the transport mechanism at the interface within a turbulent jet or the TBL via conditional fluctuations of the velocity component normal to the interface. Kovasznay *et al*. (1970) observed the existence of large-scale motions (LSMs) using the space-time correlation near the TNTI. They found that the presence of the LSMs was associated with the geometric shape of the TNTI. They also observed the presence of large-scale bursts near the TNTI that originated from near-wall small-scale eddies. Adrian *et al*. (2000) suggested that these LSMs induced from vortex packets. Westerweel *et al*. (2009) revealed the large-scale engulfment, which was generated from counter-rotating spanwise vortices. da Silva *et al*. (2014) visualized the corrugated shape of the TNTI under conditions in which large-scale vortices were located beneath the TNTI. They found that the small- and large-scale motions were closely associated with the TNTI. Although the quiescent core interface resembled the TNTI, few studies had examined the interface of the core in perspective to the TNTI.

In the present study, the interaction between the low- and high-speed structures and the core interface was examined through DNS data obtained from a turbulent pipe flow at Re_τ = 930. Various turbulent statistics were explored to analyse the similarity between TNTI and the interface of the core region. The low- and high-speed structures near the interface were classified into wall-attached and detached objects. The population and volume of the structures were examined to analyse their influence on the core interface.

NUMERICAL SIMULATION

The present study examined DNS data obtained from the work of Ahn *et al*. (2013), the turbulent pipe flow at Re_τ = 934. The Navier–Stokes equations and the continuity equation were solved to analyse the turbulent pipe flow in the fully developed incompressible flow. Following the work of Kim *et al*. (2002), the velocity and pressure were decoupled using the fractional step method. In fractional step method, The Crank–Nicolson and second-order central difference schemes were adopted over time and space to discretize the governing equations. No-slip conditions along the wall and periodic conditions along the streamwise and radial directions were applied. In the present study, x, r, and z denote the streamwise, radial, and spanwise directions, and the corresponding velocity fluctuations are u, v, and w. The wall-normal coordinate y was introduced by using $y = 1 - r$. Capital letters implied the mean quantities. Quantities with inner scaling were denoted by the superscript +. The domain length in the streamwise direction was set to 10π. The grid resolution (N_x,N_r,N_z) were set to 4097, 301, and 1025 along the streamwise, radial, and spanwise directions. The grid sizes in the wall-parallel plane were $\Delta x+ = 6.84$ and $\Delta(R\theta)+ = 5.73$. The grid spacing in the wall-normal direction varied between $\Delta y+ = 0.334$ and $\Delta y+ = +9.244$. The time step was $\Delta t+ = 0.01$.

DETECTION OF THE CORE

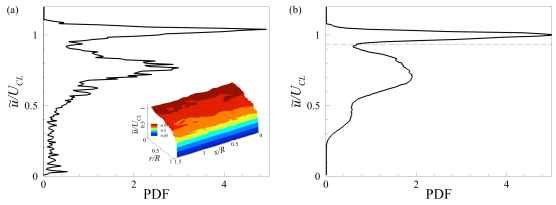

Figure 1. (a) PDF of the instantaneous streamwise velocity; (b) PDF of the modal velocity.

Figure 1(a) presents the PDF of the instantaneous streamwise velocity with a subzone over the streamwise domain length of 1.2h. The PDF of the instantaneous streamwise velocity revealed the existence of UMZs. Two peaks in Fig. 1(a) were also apparent in inset of Figure 1(a) as a large core around U_{CL} and a separate small core. The peaks in the PDF of the instantaneous streamwise velocity could be interpreted as modal velocities representing each UMZs. The modal velocities were the local maxima that appeared in the PDF of the instantaneous streamwise velocity. In the case of the PDF analysis, the result from PDF analysis varied depending on the selection of the subzone. On the other hands, the PDF obtained by averaging the modal velocities was more robust than the PDF using the instantaneous streamwise velocities. Kwon *et al*. (2014), who used experimental PIV and DNS data, had observed these properties previously. Figure 1(b) shows the PDF of the modal velocities. In PDF of the modal velocities, UMZ with a high convection velocity (around U_{CL}) was observed. This indicated that the UMZ with high convection velocity was robust. This robust UMZ was also called 'the core region' because it existed at the center of the pipe flow. The interface of the core could be defined using local minima of the PDF using modal velocity. The threshold for the core interface was located around $0.95U_{CL}$. The threshold value of the core was used to classify the turbulent pipe flow into core and non-core flows. The boundary of the core region was identified at u = 0.95UCL.

TURBULENT STATISTICS

A new coordinate system ζ was introduced to find out the statistics near the interface. Here, ζ indicates the relative distance from the core interface ($\zeta = y - y_i$).

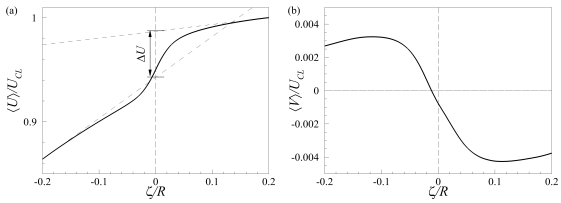

Figure 2. (a) Conditionally averaged streamwise velocity; (b) conditionally average wall-normal velocity.

Figure 2 shows the conditionally averaged velocity profile near the interface. From the streamwise velocity profile shown in Fig. 2(a), Flows with two different momentums were present. One was the high momentum region in the core region (ζ > 0) and the other was the low momentum region below the core interface (ζ < 0). On the interface between the two regions, the velocity gradient rises sharply, creating a strong shear layer. This shear layer had a characteristic similarity to the laminar superlayer present in the TNTI. The laminar superlayer contained a large amount of vorticity and the vorticity transfer due to the viscous diffusion sharply decreased as the laminar superlayer exits. Figure 2(b) represented the velocity profiles in the wall-normal direction. In this case, the downward motion of the core region and the upward motion under the core observed, and the velocity of the interface was relatively stagnated. Due to the rapid change in the velocity profiles at the interface, strong vortices resided at the interface.

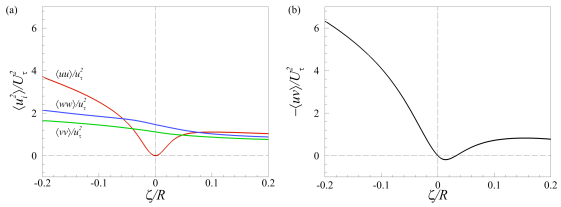

Figure 3. (a) Conditionally averaged turbulent intensities; (b) conditionally averaged Reynolds shear stress.

Figure 3(a) plots the conditional turbulence intensities near the core interface. The turbulent intensities were drastically reduced as they passed through the interface of the core. Due to the definition of the core region, the turbulent intensity in the streamwise direction became zero at the core interface. Similar trend was observed at the Reynolds shear stress in Fig. 3(b). The level of turbulence in the core region was weak and the turbulence activity in this region was not active. Due to the low level of turbulence, the core region was also called 'quiescent core region'. The laminar superlayer and a rapid decay of the turbulent intensities suggested that the interface of the core region had a similarity to TNTI.

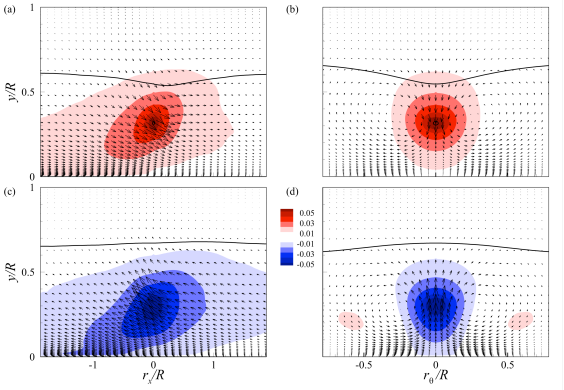

Figure 4. (a,b) Conditionally average velocity fluctuations near the high-speed structure; (c,d) conditionally average velocity fluctuations near the low-speed structure.

The conditionally averaged velocity fluctuations was performed to investigate the turbulent structure around the core interface. The conditional average expression used for this was as follows.

$$\langle u_i' \rangle_{CS}(r_x, y, r_z) = \langle u_i'(x + r_x, y, z + r_z) \,|\, CS(x, y_{ref}, z) \rangle \qquad (1)$$

Figures 4(a,b) represent the conditional average result when the high-speed structure existed around the interface. When there was the high-speed structure under the interface, the height of the interface is relatively low. In addition, it could be seen that the high-speed structure was long in the streamwise direction and short in the spanwise direction. The sweep motion was observed at the interface of the core region. For the low-speed structure shown in Fig. 4(c,d), the geometry of the low-speed structure was not significantly different from that of the high-speed structure. At the periphery of the low-speed structure, the height of the interface was relatively high and the ejection motion was observed. Figure 4(d) shows that there was a weak high-speed structure on both sides of the low-speed structure. Thus, the low- and high-speed structures around the interface were not associated with each other, but rather related to other low- and high-speed structures. The low- and high-speed structures around the interface affected the shape and statistics of the core interface.

WALL-ATTAHCED AND DETACHED OBJECTS

The percolation theory was applied to detect the low- and high-speed structures and to deal with statistics of connected structures in a random state. In order to verify the identified structure to be connected, the following equation satisfies,

$$|u(x, y, z)| > Hu(y), \qquad (2)$$

where H is a threshold value and the connection state of the structure was changed according to H.

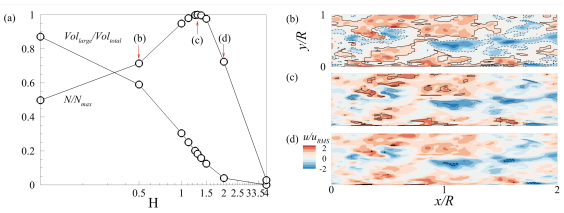

Figure 5. (a) Percolation diagram for the identification of low- and high-speed structure; (b,c,d) Instantaneous field of view depending on threshold H.

Figure 5(a) shows the percolation diagram of the equation (2). As H increased, the volume of the identified structure became smaller. Otherwise, the number of identified structures initially increased and then shrank, because the identified structures were separated and disappeared gradually. The state in which the number of identified structures was maximized, was called the percolation crisis. In this study, we selected H = 1.3, where the percolation crisis occurred.

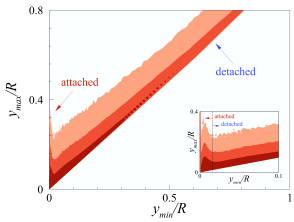

Figure 6. PDF of the maximum height and minimum height of identified low- and high-speed structure.

Figure 6 represents the PDF of the maximum height and minimum height for low- and high-speed structures, respectively. All structures were separated into the two groups. The first is a wall-attached group, which is attached in parallel to the y-axis, shown in the inset of Figure 6. The second is a wall-detached group, which is a wider band in the diagonal axis in Fig. 6. It is not easy to observe the wall-attached group in Fig. 6 because such a group exists in the very narrow strip with small y_{min}. Nevertheless, the number of the wall-attached group is not small and occupies a significant portion of the volume occupied by the low- and high-speed structures. A significant volume of the wall-attached object can affect the interface of the core region. It is necessary to investigate the effect of wall-attached and detached objects on the interface.

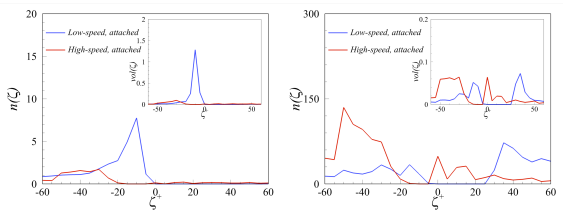

Figure 7. (a) Average number of the low- and high-speed attached structures; (b) average number of the low- and high-speed detached structures; (inset) average volume of the structures.

Figure 7 displays the average number of the attached objects as a function of the distance between the objects and the interface. Figure 7(a) shows the average number of the attached group, and the inset shows the volume of the attached group. It is seen that most of the low- and high-speed structures were located below the interface. The influence of the low-speed structure became stronger as closer to the interface. Figure 7(b) shows the results for the detached group. Considering the average number of the objects, the effect of the detached group showed stronger than the attached group. Unlike the previous results, the detached group occupied a small volume near the interface. Considering the volume in the vicinity of the interface, the attached group had a large influence on the interface. Unlike the results in the attached group, it was difficult to find a clear trend in the detached group.

CONCLUSIONS

The largest UMZ, the so-called "quiescent core region", was explored using the PDF of the modal velocity in a turbulent pipe flow with Re_τ = 934. The threshold that defined the interface of the quiescent core region was $u = 0.95U_{CL}$. The boundary of the quiescent core region was similar to the interfacial layer. In the core region above the interface, the turbulent intensities decreased drastically. An abrupt increment in the streamwise velocity occurred at the core interface, and the velocity gradient increased suddenly at the quiescent core interface. The interface of the quiescent core region was similar to the laminar superlayer in the TNTI. The interface of the quiescent core region had a corrugated shape and contained the low- and high-speed structures. The core interface formed a relatively high core height with the low-speed structure and a sweep motion. When the height of the core interface was relatively low, the high-speed structure and ejection motion were organized. The low- and high-speed structures could be classified into the wall-attached and detached groups. In the case of the wall-attached group, most of the population was concentrated below the interface of the core. The population of the wall-attached group was much smaller than that of the detached group. Although the population of the wall-attached group was relatively small, the volume of the wall-attached group was larger than that of the detached group. Due to the large volume of the wall-attached group, the wall-attached group was expected to have a strong influence on the core interface.

ACKNOWLEDGE

This work was supported by the Creative Research Initiatives (No. 2017-013369) program of the National Research Foundation of Korea (MSIP).

REFERENCE

Ahn, J., Lee, J.H., Jang, S.J., Sung, H.J., 2013, "Direct numerical simulations of fully developed turbulent pipe flows for Re_τ = 180, 544 and 934", *International Journal of Heat and Fluid Flow*, Vol. 44, pp. 222-228.

Adrian, R.J., Meinhart, C.D., Tomkins, C. D., 2000, "Vortex organization in the outer region of the turbulent boundary layer", *Journal of Fluid Mechanics*, Vol. 422, pp. 1-54.

Chauhan, K., Philip, J., de Silva, C.M., Hutchins, N., Marusic, I., 2014, "The turbulent/non-turbulent interface and entrainment in a boundary layer", *Journal of Fluid Mechanics*, Vol. 742, pp. 119-151.

Corrsin, S., Kistler, A.L., 1970, "Free-stream boundaries of turbulent flows", *NACA report 1244*.

da Silva, C.B., Hunt, J.C.R., Eames, I., Westerweel, J., 2014, "Interfacial layers between regions of different turbulence intensity", *Annual Review of Fluid Mechanics*, Vol. 46, pp. 567-590.

Kovasznay, L.S.G., Kibens, V., Blackwelder, R.F., 1970, “Large-scale motion in the intermittent region of a turbulent boundary layer”, *Journal of Fluid Mechanics*, Vol. 41, pp. 283-325.

Kwon, Y.S., Philip, J., de Silva, C.M., hutchins, N., Monty, J.P., 2014, “The quiescent core of turbulent channel flow”, *Journal of Fluid Mechanics*, Vol. 751, pp. 228-254.

Kim, K., Baek, S.J., Sung, H.J., 2002, “An implicit velocity decoupling procedure for the incompressible Navier-Stokes equations”, *International Journal for Numerical Methods in Fluids*, Vol. 38 (2), pp. 125-138.

Meinhart, C.D., Adrian, R.J., 1995, “On the existence of uniform momentum zones in a turbulent boundary layer”, *Physics of. Fluids*, Vol. 7, pp. 694-696

Westerweel, J., Fukushima, C., Pedersen, J.M., Hunt, J.C.R., 2005, “Mechanics of the turbulent-nonturbulent interface of a jet”, *Physical Review Letters*, Vol. 95, 174501.

Westerweel, J., Fukushima, C., Pedersen, J.M., Hunt, J.C.R., 2009, “Momentum and scalar transport at the turbulnt/non-turbulent interface of a jet”, *Journal of Fluid Mechanics*, Vol. 631, pp. 199-230.